2022

Effect Of Heat Exchanger Size On Subcooling Control In Residential Air Conditioning Systems

Bruno Yuji Kimura de Carvalho

Pega Hrnjak

Effect Of Heat Exchanger Size On Subcooling Control In Residential Air Conditioning Systems

Bruno Yuji Kimura DE CARVALHO[1]*, Pega HRNJAK[1,2]*

[1]ACRC, University of Illinois at Urbana-Champaign,
Urbana, Illinois, USA
brunoykc@illinois.edu

[2]Creative Thermal Solutions Inc.
Urbana, Illinois, USA
pega@illinois.edu

* Corresponding Author

ABSTRACT

With the increasing pressure on reducing the environmental impact of air conditioning and heat pump systems alternative solutions are required to maintain or increase energy efficiency while also decreasing the overall carbon footprint of such systems. This paper will focus on experimental and model evaluation of heat exchanger (HX) size effect on the control of subcooling in residential air conditioning systems.

Two separate systems are investigated: a high-efficiency system with large heat exchangers, variable-capacity compressor, and thermostatic valve; and a lower efficiency system with smaller heat exchangers, fixed speed compressor, and piston-orifice tube. Experimental results showed that both systems improved with subcooling control with relative increases in COP from +4.7% to +8.9% for the large-HX system and from +4.3 to +14.2% in the small-HX system. Subcooling control also increased capacity for both systems ranging from +5.3% to +15.6%. With a more significant overall improvement in performance for the small-HX system because its baseline used a fixed-expansion device which suffers a decrease in efficiency when operating outside of the rating condition. A system model was developed and predicted for a system using the same variable capacity compressor that the COP-maximizing subcooling is a function of both heat exchanger size and capacity, with the latter having a more pronounced effect on it. The system with heat exchangers 5 times smaller showed an increase in COP-maximizing subcooling of only 1-2 K for residential applications at the A rating condition. When the capacity was increased from 3 kW to 7 kW COP-maximizing subcooling rose from 2-3 K to 6-8 K for both small and large heat exchanger systems.

The control strategy proposed based on a linear function of the difference between condenser saturation temperature and condenser air inlet temperature agrees well with the experimental results for both systems. A simple control scheme was used to control subcooling by regulating the refrigerant flow with an electronic expansion valve and maximize the COP.

1. INTRODUCTION

Subcooling can provide an improvement in performance for most vapor compression cycles. By subcooling the liquid it's possible to reduce the throttling losses as a lower temperature reduces the entropy generation on this near isenthalpic process. Domanski (1995) simplified relative loss in capacity from the throttling process into equation 1. It is important to note that the only factors that influence this loss are based on the conditions (evaporation and condensation temperatures) and on the fluid properties. If the conditions are kept the same throttling losses will be a function of only the refrigerants thermophysical properties. Pottker and Hrnjak (2015a) came to a similar conclusion regarding the improvements obtained from subcooling in an ideal refrigeration cycle.

$$\frac{Q_{exp}}{Q_C} = \frac{\frac{1}{COP_C} - \ln\frac{T_{cr,sat}}{T_{er,sat}}}{\frac{h_{er,fg}}{T_{er,sat}\bar{c}_{p,cr.l}} - \ln\frac{T_{cr,sat}}{T_{er,sat}}} \quad (1)$$

The effect of system charge on the subcooling is well known and has been used to properly charge systems by most manufacturers. Choi and Kim (2002 and 2004) investigated the effect of refrigerant charge on the performance of R22/ R407C systems, obtaining different optimal subcooling values for the refrigerants tested. Primal and Lundqvist (2005) and Corberan et al. (2008) both worked on the charge effect in R290 heat pumps and obtained an optimal subcooling as a function of the charge in the system. Hwang et al. (2007) compared the R290, R404A and R410A for walk-in refrigeration systems and found different optimum subcooling values (at their optimum charges) for each system with their respective optimized condenser circuitry and scroll compressor.

Pottker and Hrnjak (2015ab) investigated the improvement from subcooling compared to zero subcooling in air conditioning systems through both modeling and experimentally. The subcooling was controlled by refrigerant charge and the authors found that the COP-maximizing subcooling is independent of the refrigerant, but the benefit from subcooling is linked to the refrigerant thermophysical properties, being inversely proportional to the latent heat of vaporization at the evaporation pressure and directly proportional to the saturated liquid specific heat. Their analysis, however, does not reflect how focusing on active subcooling control can be beneficial over more traditional expansion devices which focus on controlling evaporator superheat.

Xu and Hrnjak (2014) also investigated the use of subcooling control through a RAC R410-A system experimentally and using validated. The authors showed that the COP improvement is inversely proportional to the condenser size. They showed that control based on a linear function of ΔT_{cra}, shown in equation 2, can provide an acceptable control strategy. However, no theoretical backing behind the selection of this control parameter was given besides its capability to represent condenser size/capacity.

$$\Delta T_{cra} = T_{cr.sat} - T_{cai} \quad (2)$$

Pitarch et al. (2017a, b, c) and Hervas-Blasco et al. (2018 and 2019) have also studied subcooling control in heat pump water heaters using R290 and concluded that optimal subcooling may be obtained as a function of the temperature lift of the secondary fluid or a fixed pinch point temperature difference, or approach, may be used as a simpler control strategy to keep performance close to optimal levels. The authors observed that this parameter was able to approximately keep the system at it HPF-maximizing subcooling at varying conditions. Experimental results corroborating the benefit from COP-maximizing subcooling and no evaporator superheat combined were presented by de Carvalho and Hrnjak (2020ab).

This paper will investigate theoretically the use of condenser variables to the COP-maximizing subcooling and experimentally evaluate the impact of subcooling control on the performance of a R410-A air conditioning. A comparison the same system using a thermostatic valve will also be presented along with a comparison of SEER improvements.

2. THEORETICAL ANALYSIS

The fundamental mechanism behind an efficiency-maximizing subcooling is the increase in specific capacity from decreasing expansion inlet enthalpy while simultaneously increasing condensation pressure as subcooling uses up some of the two-phase heat transfer area in the condenser which reduces its overall UA value. And due to the developing regulations focusing on the reduction of HVAC system's environmental impact it's important to determine the potential benefit from subcooling for current and possible future refrigerant fluids used in residential, mobile, commercial, and industrial applications.

Pottker and Hrnjak (2012) have previously evaluated the theoretical potential of subcooling control in cooling operation by comparing the relative increase in specific capacity (qe) and specific compression work if subcooling is increased by 6 K versus zero subcooling for an ideal cycle with a fixed evaporator pressure and outlet quality. A similar approach will be presented with further analysis into the relative increase in COP.

Figure 1 shows the main variables used in this simple analysis. An increase of 6 K in subcooling will be assumed to raise the condensation temperature $\Delta T_{c,sat}$ by 1 K, while the temperature at the expansion inlet is reduced by a $\Delta T_{c,out}$ vale of 5 K. The evaporation temperature is kept constant, and the evaporator outlet/compressor suction quality is set at 1. The relative increases $\frac{\Delta q_e}{q_e}$, $\frac{\Delta w}{w}$, and $\frac{\Delta COP}{COP}$ are shown in equations 3,4 and 5, respectively. The approximation of relative increase in cooling capacity (Equation 6) by Pottker and Hrnjak (2012) is also used to compare several refrigerants.

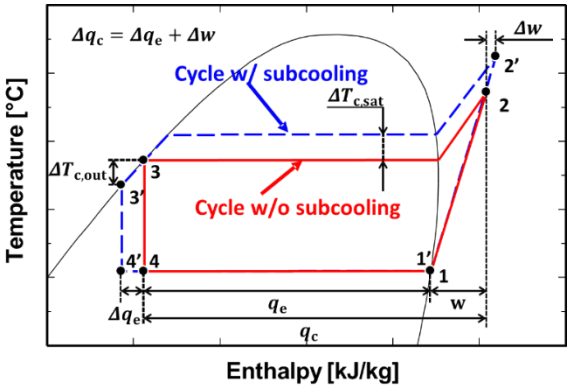

Figure 1: Normalized subcooling/two-phase heat transfer areas and two-phase heat transfer vs condenser subcooling

$$\frac{\Delta q_e}{q_e} = \frac{h_3 - h_{3'}}{h_1 - h_3} \tag{3}$$

$$\frac{\Delta w}{w} = \frac{h_{2'} - h_2}{h_2 - h_1} \tag{4}$$

$$\frac{\Delta COP}{COP} = \frac{COP'}{COP} - 1 = \frac{\frac{q_e + \Delta q_e}{w + \Delta w}}{\frac{q_e}{w}} - 1 = \frac{1 + \frac{\Delta q_e}{q_e}}{1 + \frac{\Delta w}{w}} - 1 \tag{5}$$

$$\frac{\Delta q_e}{q_e} \cong \frac{\Delta T_{c,out}}{\frac{h_{fg,e}}{c_{pl,c}} + (T_c - T_e)_{sat}} \tag{6}$$

Table 1 shows the results for this analysis including relative changes for several refrigerants. The relation's trend in equation 6 is validated by this analysis, although some small deviations on the relative COP increase occur, possibly due to a combination of other minor effects from less relevant properties, as shown in figure 2. Ammonia (R717) shows almost no benefit from subcooling due to its high enthalpy of vaporization while R1234yf has the highest improvement because its enthalpy of vaporization is 12.9% of R717's while its liquid isobaric specific heat is 30% of R717's leading to a decrease in $\frac{h_{fg,e}}{c_{pl,c}}$ of 59.0%.

Table 1: Effect of thermophysical properties of different refrigerants on the relative change in performance characteristics in an ideal cycle as subcooling is increased

Refrigerant	$c_{\mathrm{pl,c}}$	$h_{\mathrm{fg,e}}$	$h_{\mathrm{fg,c}}$	$\frac{h_{\mathrm{fg,e}}}{c_{\mathrm{pl,c}}}$	$\frac{\Delta w}{w}$	$\frac{\Delta q_{\mathrm{e}}}{q_{\mathrm{e}}}$	$\frac{\Delta COP}{COP}$
[-]	$\left[\frac{\mathrm{kJ}}{\mathrm{kg\,K}}\right]$	$\left[\frac{\mathrm{kJ}}{\mathrm{kg}}\right]$	$\left[\frac{\mathrm{kJ}}{\mathrm{kg}}\right]$	[K]	[%]	[%]	[%]
R717	5.0	1244	1076	232	2.5	2.8	0.3
R22	1.4	201	161	131	2.4	5.4	2.9
R32	2.3	307	224	116	2.5	5.7	3.2
R600a	2.6	350	305	127	2.2	6.1	3.8
R454B	2.1	254	185	104	2.4	6.7	4.2
R134A	1.5	195	158	115	2.2	6.6	4.3
R290	3.0	368	296	111	2.2	6.8	4.5
R407C	1.7	205	157	105	2.3	7.0	4.6
R410A	2.1	215	148	88	2.4	8.0	5.6
R1234yf	1.5	160	127	95	2.1	8.5	6.3

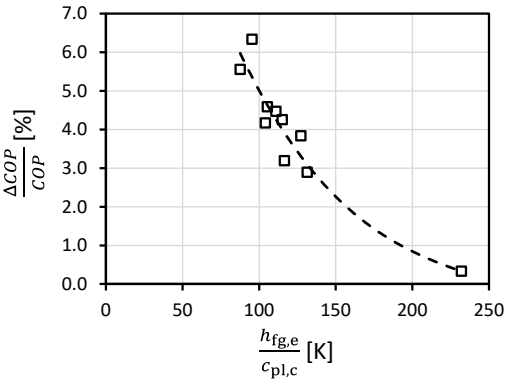

Figure 2: Relative performance increase trends down as the ratio between latent heat of vaporization and liquid specific heat increases

The mechanism through which subcooling defines a maximum efficiency point for a system with a fixed evaporator outlet state were presented by Carvalho and Hrnjak (2020a) along with the definition of a linear control curve based on the difference between condenser saturation temperature and air inlet temperatures, shown in equation 7.

$$\Delta T_{SC}\left(COP_{maximizing}\right) \cong a\Delta T_{cra}\,(K) + b \tag{7}$$

The trade between heat transfer area dedicated to subcooling and two-phase decrease the condenser's UA and the enthalpy at the inlet of the expansion device, with the former causing an increase in compression work as the condensation pressure rises, and the latter increasing specific refrigerating effect. These effects vary at different rates: the compression work follows an ascending quadratic slope while the refrigerating effect is attenuated as subcooling increases because as the high-side pressure increases it pushes the saturation line forward and subcooling effectiveness is limited by the air inlet temperature. The combination of these two consequences lead to an optimum condenser subcooling defining a maximum COP. Figure 3 shows the results of a condenser model representing the pressure and enthalpy at the expansion device inlet as subcooling is increased. Initially subcooling is easily achieved by the condenser, but gradually the shifting saturation point along with the minimum temperature defined by the air inlet diminish the cooling effect obtained through subcooling.

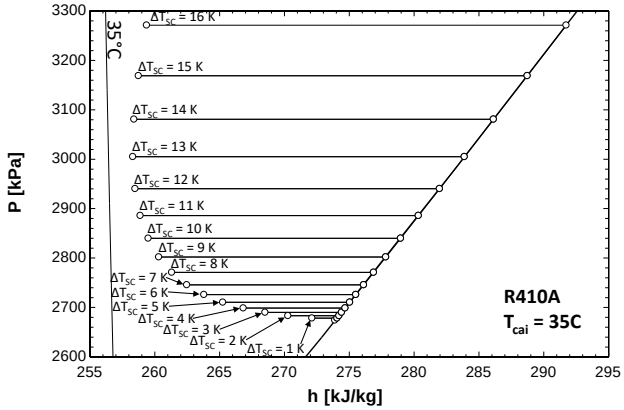

Figure 3: Effect of subcooling on the enthalpy at the expansion device inlet and condensation pressure for R410A.

3. FACILITY

To evaluate the improvement from subcooling control in residential air-conditioning systems two different system were used in this work: a high-SEER (22-24) (Seasonal Energy Efficiency Ratio) R410A system using a thermostatic valve, and a low-SEER (12-14) R410A system with piston orifice tube. Both facilities follow a similar setup shown in figure 4, comprised of two environmental chambers to emulate both indoor and outdoor conditions.

4WV: 4-way valve
ABL: Air blender
ACC: Accumulator
AIR: Air
BL: Blower
CC: Charge compensator
CD: Condenser
CP: Compressor
DP: Differential pressure transducer
DPS: Dew-point sensor
EGC: Ethylene glycol chiller
EGHX: Ethylene glycol heat exchanger
ERH: Electric resistance heater
EV: Evaporator
EXV: Electronic expansion valve
FN: Flow nozzle
MF: Muffler
MFM: Mass flow meter
P: Absolute pressure transducer
SI: Steam injection
T: Type-T thermocouple
TCG: Thermocouple grid
TXV: Thermostatic expansion valve
VFD: Variable frequency drive

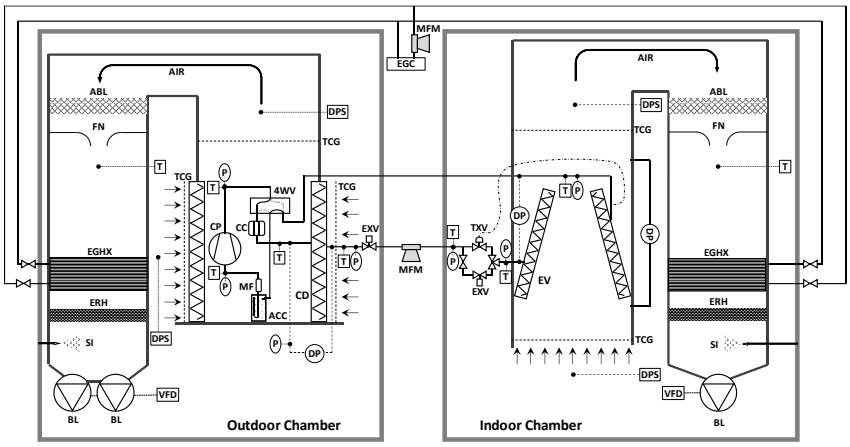

Figure 4: Layout of facility for performance evaluation

Air-side, refrigerant-side and chamber-balance capacity calculations have an expanded uncertainty of ±4% and COP uncertainty is calculated to be ±5% using EES (Klein, 2021). The oil circulation ratio was measured for the low-SEER system to be 0.4%, this is used to correct the refrigerant side calculations. Temperature on the chambers is controlled through an ethylene glycol chilled loop along with PID controlled electric heaters. The high-SEER facility uses wind-tunnels for the energy balance determination in both indoor and outdoor heat exchangers and humidity is controlled through steam injection only in the outdoor chamber. The low-SEER facility only employs a wind tunnel for its indoor unit and both chambers are humidity controlled using an electric-heated steamer.

The high-SEER and low-SEER systems' heat exchanger specifications and air flow rates are shown in table 2, respectively. Both systems are rated as 2-ton (7 kW), with the high-SEER system using a variable speed (30-120 Hz) scroll compressor with 21.5 cm^3 displacement volume, while the low-SEER system has a fixed speed (58.33 Hz) scroll compressor with 19.0 cm^3 displacement volume. It's important to note that the higher-efficiency system has 5.5 and 4.5 times the air-side heat transfer area than the lower-efficiency system for the outdoor and indoor heat exchangers, respectively.

Table 2: Residential system heat exchanger specifications

System	High-SEER system		Low-SEER system	
Heat exchanger (HX)	Outdoor HX	Indoor HX	Outdoor HX	Indoor HX
Description	2 rows, 8 circuits, 20 fpi	2 slabs, 3 staggered rows, 8 circuits, 14.5 fpi	1 row, 6 circuits, 18.8 fpi	2 slabs, 3 staggered rows, 3 circuits, 11.4 fpi
Face area	2.81 m^2	0.689 m^2	1.844 m^2	0.344 m^2
Core depth	0.038 m	0.056 m	0.025 m	0.055 m
Core volume	0.1068 m^3	0.03858 m^3	0.047 m^3	0.019 m^3
Air side area	153.53 m^3	40.1 m^3	28.11 m^2	8.95 m^3
Refrigerant side area	4.61 m^3	2.39 m^3	1.45 m^2	0.91 m^3
Air flow rate	1.08 m^3/s	0.42 m^3/s	~1.18 m^3/s	0.41 m^3/s
Material	Aluminum straight fins, copper tubes, vapor line O.D. = 22 mm / liquid line O.D. = 9.5 mm		Aluminum louvered fins, copper tubes, vapor line O.D. = 22 mm / liquid line O.D. = 9.5 mm	

4. RESULTS AND DISCUSSION

4.1 Effect of subcooling control compared with more conventional expansion devices

To compare the high-SEER and low-SEER systems the AHRI 210/240 rating conditions A, C (dry B condition) were used. The high-SEER tests selected represent the maximum capacity tests to provide a close comparison to the low-SEER testing conditions. Also, the low-SEER system capacity was corrected by adding the indoor fan power to it to account for the lack of indoor fan on the high-SEER system facility. The high-SEER system ran at a dry A condition while the low-SEER system was able to operate at the original wet condition. At each condition the electronic expansion valve will be used to sweep through the subcooling and define the COP-maximizing subcooling as well as observe how the systems behave as the condenser subcooling is varied with a fixed refrigerant charge. The results can be then compared to the baseline systems using their respective refrigerant charges.

Figure 5 shows the COP (a), capacity (b) and compressor power (c) for both the high-SEER system and the low-SEER system. The high-SEER test was performed in a dry condition which should reduce its overall performance slightly. The relative COP improvement for the low-SEER system is lower due to the wet test conditions which seem to benefit the baseline with dryout in the evaporator. This happens because at high evaporator superheat in wet test conditions the dehumidification (or latent heat transfer) is increased with lower evaporation temperatures which diminishes the losses from not having fully flooded evaporators. The resulting effect can be seen in figure 5b where the baseline capacity is higher even when operating with lower subcooling values than the SC control. Therefore, this effect is important to consider when using subcooling control to maximize COP without sacrificing the dehumidification capacity of the system.

T-h diagrams comparing both baselines and COP-maximizing subcooling are shown in figure 6. In here it's evident how the COP-max. SC is higher for the low-SEER system due to its much lower condenser UA, or higher condenser LMTD which drives the condensation pressure higher as subcooling is increased. The ΔT_{cra} values corroborate the trend obtained theoretically by Carvalho and Hrnjak (2020a).

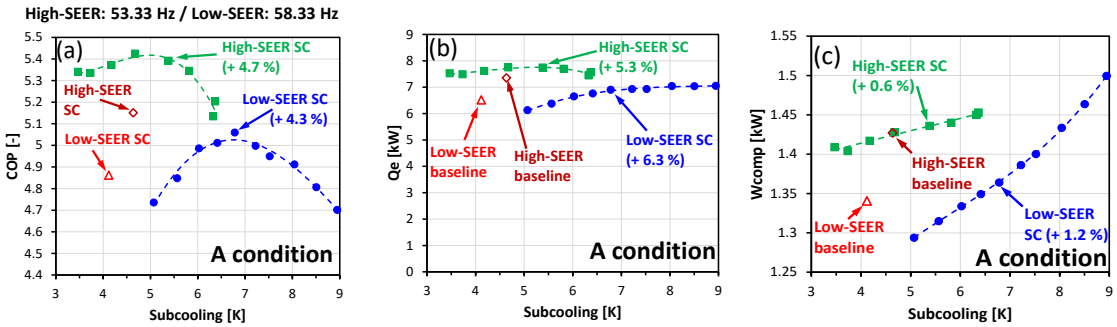

Figure 5: COP (a), Q_e (b) and W_{comp} (c) results for the A/C A condition

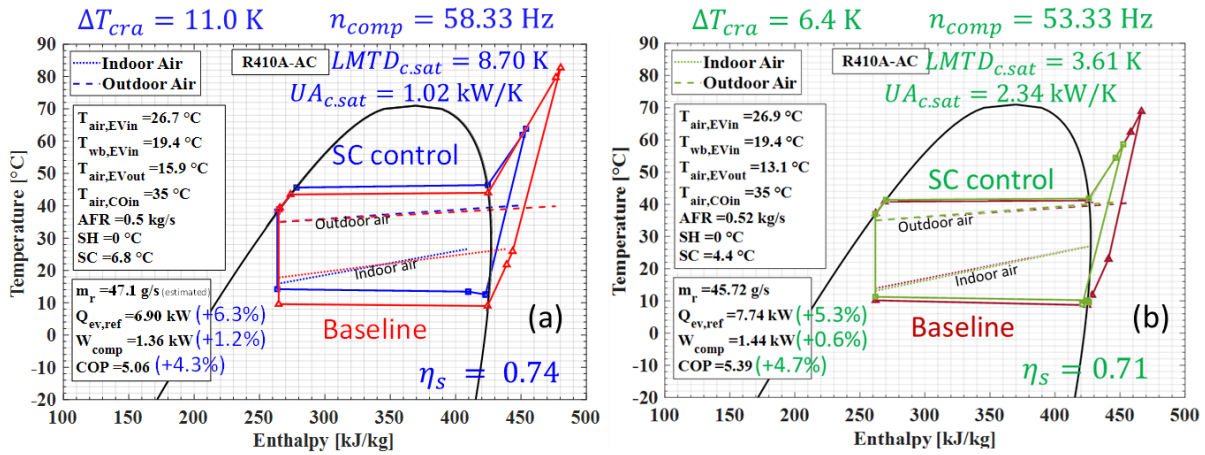

Figure 6: T-h diagrams for the low-SEER system (a), high-SEER system (b), baselines vs. COP-maximizing SC for the A condition

To verify if the dehumidification penalizes subcooling control in the low-SEER system condition C was tested. In this case figure 7 shows that the low-SEER system with SC control boosts COP by 14.2 % because there's no increased latent heat as the evaporation temperature decreases, and the baseline piston tube can only be optimally designed for a single condition (in most cases the rating condition A). This condition also shows that compressor speed, or capacity, matter more than load to define the COP-max. subcooling. The ΔT_{cra} values for this condition are similar to the A condition, 10.9 K and 6.4 K for the Small Low-SEER and Large High-SEER systems, respectively, thus resulting in no change for COP-max. subcooling.

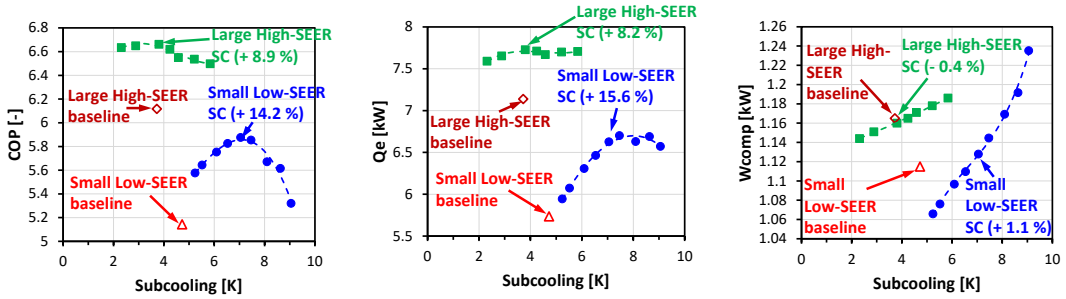

Figure 7: COP (a), Q_e (b) and W_{comp} (c) results for the A/C A condition

Following AHRI 210/240 it's possible to calculate the improvement from subcooling control over the baseline systems. Table 4.6 shows the region IV SEER for both high and low SEER systems tested. The SEER shows a greater relative improvement with the low-SEER system due to its use of orifice piston tubes for the baseline. Because these devices provide a fixed restriction expansion their operation is only optimized for a single condition. Calculation for each system differs slightly as the high-SEER system uses a variable capacity compressor, requiring maximum and minimum capacity testing, while the low-SEER system only needs half the data points. The default cycling degradation coefficient of 0.25 was used for both systems in these calculations.

Table 3: SEER results for baseline and SC-controlled low-SEER and high-SEER systems

SEER			
Baseline High-SEER	**SC control High-SEER**	**Baseline Low-SEER**	**SC control Low-SEER**
22.5	**24.4 (+8.4%)**	**12.6**	**13.9 (+10.3%)**

4.2 Subcooling control scheme

Using the recorded data from both systems along with other COP-maximizing subcooling values for the high-SEER system a control curve can be defined following the scheme shown in equation 7. Figure 8 shows the COP-maximizing subcooling curve as a function of ΔT_{cra}. The behavior perfectly mirrors the expected control curve defined by equation 7 corroborating its application in providing maximum efficiency for residential air-conditioning systems. This control could be applied using three temperature sensors, as shown in figure 8.

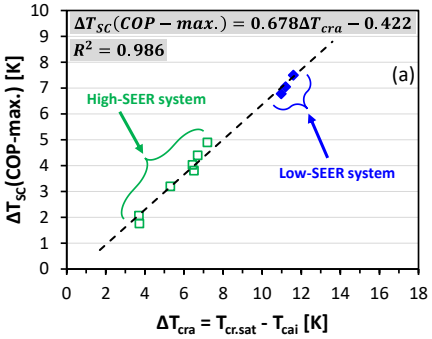

Figure 8: COP-maximizing subcooling control curve as a function of ΔT_{cra}

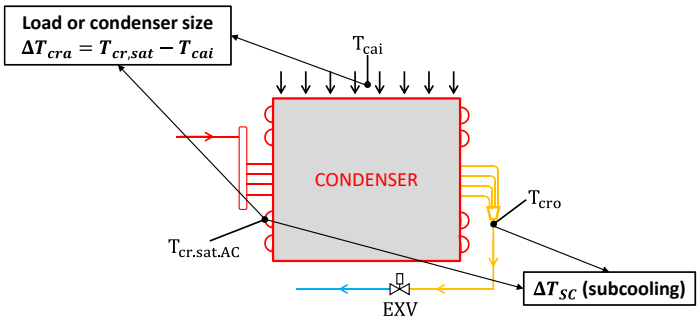

Figure 9: Sensor placement for subcooling control in A/C systems

4.3 System model analysis on the effect of heat exchanger size

To further evaluate the potential improvement of subcooling control in other systems with different refrigerants and components a generalized model has been developed in python using a CoolProp (Bell et al, 2014) wrapper with REFPROP (Lemmon et al 2018) to calculate thermophysical properties. The model uses an ε-NTU method for the heat exchangers and a 37-coefficient semi-empirical compressor correlation for the High-SEER variable capacity compressor with Rice and Dabiri's (1981) correction. Table 4 shows the correlations used in the system model.

Table 4: Correlations used in the system model

System fluid / components		**Correlations**
Refrigerant	Single phase HTC	Gnielisnki, 1976
	Condensation HTC	Dobson & Chato, 1998
	Evaporation HTC	Gungor & Winterton, 1986
	Single phase DP	Churchill, 1977
	Two-phase DP	Friedel, 1979
	Void fraction	Rouhani & Axelsson, 1970
Air	Air-side fin-tube HTC	Chang and Wang, 2000
	Air-side fin-tube DP	Chang and Wang, 2000

Using the geometry of both the High-SEER HX and the Low-SEER HX a comparison was made using the model. The capacity was set at 3, 5 and 7 kW by controlling the compressor speed and the systems were compared with a fixed evaporator superheat of 4 K and fixed evaporator outlet quality of 0.92 (to emulate a partially filled accumulator. The rating condition A was used to evaluate the performance here. Figure 10 shows the COP vs subcooling for 3 capacities, both HX sizes and two different evaporator outlet conditions. The trend follows the predictions by Carvalho and Hrnjak (2020a) with increasing COP-max. subcooling as HX size is decreased or as the capacity is increased. The effect of heat exchanger size is not pronounced for residential systems as the Low-SEER system has approximately 1/5 of the air-side surface area but only results in a 1-2 K increase in COP-max. subcooling. The relative improvement of the x_{ero} = 0.92 COP-maximizing subcooling to SH_{ero} = 4 K with ΔT_{SC} = 0 K shows similar values for both systems at 5 kW and 7 kW at around +12.5%, with a decrease in performance improvement for the Low-SEER system at 3 kW at +6.8%.

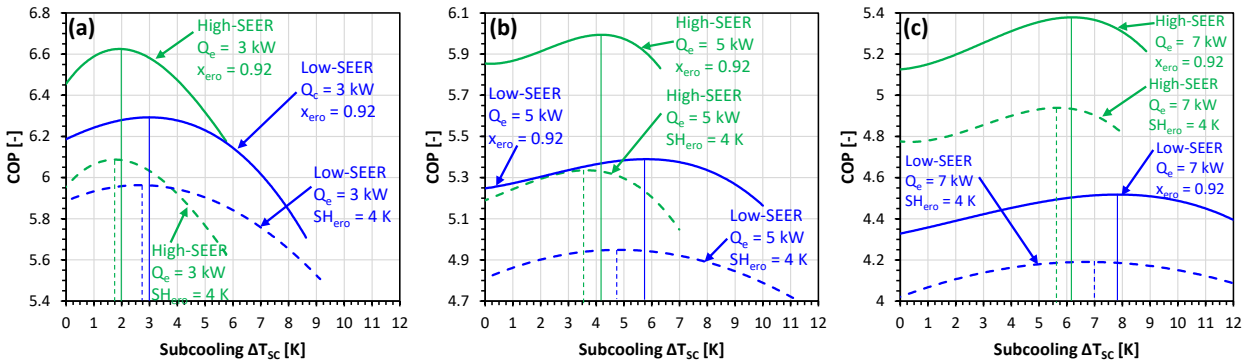

Figure 10: COP behavior vs. subcooling model results for both systems using the same variable speed compressor at 3 kW (a), 5 kW (b) and 7 kW (c) with two different evaporator outlet states (x_{ero} = 0.92 and SH_{ero} = 4 K)

5. CONCLUSIONS

The theoretical analysis showed that the benefit from subcooling is dependent on the ratio of enthalpy of vaporization to liquid isobaric specific heat. Low-capacity refrigerants, such as R1234yf, have a higher relative COP improvement due to subcooling. The mechanism through which subcooling provides a maximum efficiency is based on the minimization of the enthalpy at the expansion device inlet, based on the effectiveness of the subcooling region and condenser air inlet temperature, while simultaneously increasing the condenser saturation pressure as the two-phase heat transfer area is decreased in the condenser. Two off-the-shelf residential air conditioning system were used to evaluate the overall COP and SEER and define if heat exchanger size has a significant impact on subcooling control

improvement. Experimental results showed that both systems improved with subcooling control with relative increases in COP from +4.7% to +8.9% for the large-HX system and from +4.3 to +14.2% in the small-HX system. Subcooling control also increased capacity for both systems ranging from +5.3% to +15.6%. The small-HX Low-SEER system showed a higher SEER improvement of +10.3% compared to +8.4% for the High-SEER system, but the increase in efficiency can be attributed to its baseline usage of a fixed expansion device. For residential air conditioning systems, the effect of HX size on COP improvement from subcooling control is not significant when considering that the heat exchanger's air-side heat transfer area of the Low-SEER system was approximately 1/5 of the High-SEER system.

Control based on ΔT_{cra} was found to agree well experimentally for the cooling operation regardless of the system assessed, meaning a unified control scheme could be used to maximize efficiency in residential air-conditioning applications. The system model corroborates the effect of HX size on subcooling control observed experimentally, with similar performance improvement for 5 and 7 kW using the same compressor model, and a lower efficiency enhancement for the Low-SEER system at 3 kW.

NOMENCLATURE

A/C	Air conditioning	
COP	Coefficient of performance	(–)
EXV	Electronic expansion valve	
h	Enthalpy	(kJ kg-1)
m	Mass flow rate	(kg s-1)
P	Pressure	(kPa)
q	Specific cooling capacity	(kW kg^{-1})
Q	Capacity	(kW)
RAC	Residential air conditioning	
SC	Subcooling	
SEER	Seasonal energy efficiency ratio	
SH	superheat	
T	Temperature	(°C or K for differences)
TXV	Thermostatic expansion valve	
x	Refrigerant quality	(-)
w	Specific work	(kW kg-1)
W	Work/Power	(kW)

Subscript

a	air (subscript)
c	condenser (subscript)
comp	compressor (subscript)
e	evaporator (subscript)
i	inlet (subscript)
o	outlet (subscript)
r	refrigerant (subscript)
sat	saturation (subscript)
SC	subcooling (subscript)
SH	superheat (subscript)

REFERENCES

Bell, I. H., Wronski, J., Quoilin, S., & Lemort, V. (2014). Pure and Pseudo-pure Fluid Thermophysical Property Evaluation and the Open-Source Thermophysical Property Library CoolProp. Industrial & Engineering Chemistry Research, 53(6), 2498–2508. doi:10.1021/ie4033999

Churchill, S.W. (1977). Friction-factor equation spans all fluid-flow regimes, Chem. Eng. 84 (24), 91-92.

Choi, J., & Kim, Y. (2002). The effects of improper refrigerant charge on the performance of a heat pump with an electronic expansion valve and capillary tube. Energy, 27(4), 391–404. doi:10.1016/s0360-5442(01)00093-7

Choi, J., & Kim, Y. (2004). Influence of the expansion device on the performance of a heat pump using R407C under a range of charging conditions. International Journal of Refrigeration, 27(4), 378–384. doi:10.1016/j.ijrefrig.2003.12.002

Corberán, J. M., Martínez, I. O., & Gonzálvez, J. (2008). Charge optimisation study of a reversible water-to-water propane heat pump. International Journal of Refrigeration, 31(4), 716–726. doi:10.1016/j.ijrefrig.2007.12.011

de Carvalho, B.Y.K., Hrnjak, P. (2020a). Experimental and Theoretical Analysis of Subcooling Control in Residential Air Conditioning Systems. *Proceedings of the 18th International Refrigeration and Air Conditioning Conference at Purdue, West Laffayette, USA* (2653).

de Carvalho, B.Y.K., Hrnjak, P. (2020b). Effect of Subcooling Control on Residential Heat Pump Systems' Performance. *Proceedings of the 18th International Refrigeration and Air Conditioning Conference at Purdue, West Laffayette, USA* (2654).

Dobson, M. K., and Chato, J. C. (1998). Condensation in smooth horizontal tubes. ASME J. Heat Transfer, 120, pp. 193-213.

Domanski, P. (1995), Theoretical evaluation of the vapor compression cycle with a liquid-line/suction-line heat exchanger, economizer, and ejector (NISTIR 5606), NIST Interagency/Internal Report (NISTIR), National Institute of Standards and Technology, Gaithersburg, MD, [online], https://doi.org/10.6028/NIST.IR.5606 (Accessed September 14, 2021)

Friedel, L. (1979). Improved friction pressure drop correlation for horizontal and vertical two-phase pipe flow. *Proc. of European Two-Phase Flow Group Meet., Ispra, Italy, 1979*.

Gnielinski, V. (1976). New equations for heat and mass transfer in turbulent pipe and channel flow. *Int. Chem. Eng.*, *16*(2), 359-368.

Gungor, K. E., & Winterton, R. H. S. (1986). A general correlation for flow boiling in tubes and annuli. *International Journal of Heat and Mass Transfer*, *29*(3), 351-358.

Hervas-Blasco, E., Pitarch, M., Navarro-Peris, E., & Corberán, J. M. (2018). Study of different subcooling control strategies in order to enhance the performance of a heat pump. International Journal of Refrigeration, 88, 324–336. doi:10.1016/j.ijrefrig.2018.02.003

Hervás-Blasco, E., Navarro-Peris, E., Barceló-Ruescas, F., & Corberán, J. M. (2019). Improved water to water heat pump design for low-temperature waste heat recovery based on subcooling control. International Journal of Refrigeration. doi:10.1016/j.ijrefrig.2019.06.030

Pitarch, M., Navarro-Peris, E., Gonzálvez-Maciá, J., & Corberán, J. M. (2017a). Evaluation of different heat pump systems for sanitary hot water production using natural refrigerants. Applied Energy, 190, 911–919. doi:10.1016/j.apenergy.2016.12.166

Pitarch, M., Hervas-Blasco, E., Navarro-Peris, E., Gonzálvez-Maciá, J., & Corberán, J. M. (2017b). Evaluation of optimal subcooling in subcritical heat pump systems. International Journal of Refrigeration, 78, 18–31. doi:10.1016/j.ijrefrig.2017.03.015

Pitarch, M., Navarro-Peris, E., Gonzálvez-Maciá, J., & Corberán, J. M. (2017c). Experimental study of a subcritical heat pump booster for sanitary hot water production using a subcooler in order to enhance the efficiency of the system with a natural refrigerant (R290). International Journal of Refrigeration, 73, 226–234. doi:10.1016/j.ijrefrig.2016.08.017

Pottker, G. (2012). Potentials for COP increase in vapor compression systems. University of Illinois at Urbana-Champaign.

Pottker, G., & Hrnjak, P. (2015a). Effect of the condenser subcooling on the performance of vapor compression systems. International Journal of Refrigeration, 50, 156–164. doi:10.1016/j.ijrefrig.2014.11.003

Pottker, G., & Hrnjak, P. (2015b). Experimental investigation of the effect of condenser subcooling in R134a and R1234yf air-conditioning systems with and without internal heat exchanger. International Journal of Refrigeration, 50, 104–113. doi:10.1016/j.ijrefrig.2014.10.023

Radermacher, R., Yang, B., & Hwang, Y. (2007). Integrating alternative and conventional cooling technologies. Ashrae Journal, 49(10), 28-35.

Rouhani, S. Z., & Axelsson, E. (1970). Calculation of void volume fraction in the subcooled and quality boiling regions. *International Journal of Heat and Mass Transfer*, *13*(2), 383-393.

Wang, C. C., Chi, K. Y., & Chang, C. J. (2000). Heat transfer and friction characteristics of plain fin-and-tube heat exchangers, part II: Correlation. *International Journal of Heat and mass transfer*, *43*(15), 2693-2700.

Xu, L., Hrnjak, P.S. (2014). Potential of controlling subcooling in residential a/c system. International Refrigeration and Air Conditioning Conference, Purdue University, West Lafayette, IN, United States.

ACKNOWLEDGEMENT

This work was supported by the Air Conditioning and Refrigeration Center at the University of Illinois at Urbana-Champaign. Support from ACRC members and sponsors are gratefully acknowledged.